Voltage-Mode CFTA-C Third-Order Elliptic Low-Pass Filter Design and Optimization Using Signal Flow Graph Approach

Norbert Herencsar[1], Jaroslav Koton[1], Jiun-Wei Horng[2], Kamil Vrba[1], Martin Venclovsky[1]
[1]*Department of Telecommunications, Brno University of Technology,*
Technicka 3082/12, 616 00 Brno, Czech Republic
[2]*Department of Electronic Engineering, Chung Yuan Christian University,*
Chung Li District, Taoyuan City, 32023, Taiwan
herencsn@feec.vutbr.cz

***Abstract*—In this work, two active only grounded-C equivalents of third-order voltage-mode (VM) elliptic low-pass (LP) LC ladder prototype are proposed. As active building blocks (ABBs) the recently introduced current follower transconductance amplifier (CFTA) were used. The first active only grounded-C LP filter employing eight CFTAs was proposed by interconnecting CFTA-based active equivalent sub-blocks of passive components, where one of the low-impedance input terminals is not used. Since such feature may cause some noise injection into the proposed circuit, the proposed filter was optimized using Mason-Coates' signal flow graph approach. In several steps the number of ABBs was reduced by two and the unused input terminal was eliminated. The performance of the novel and optimized active only grounded-C third-order VM elliptic LP filter was tested experimentally using the readily available UCC-N1B integrated circuit.**

***Index Terms*—Active equivalent, analog filters, current follower transconductance amplifier, CFTA, experiments, Mason-Coastes signal flow graph, LC ladder filter, optimization, passive prototype.**

I. INTRODUCTION

Analog filters have wide area of applications in instrumentation, automatic control, and communication systems. It is well-known that filters with good frequency selectivity have to be of the order higher than two. During the last decades it was shown that LC ladder structures have minimum sensitivity to component variations in the frequency band of interest. Thus, the performance of these types of passive filter structures is very reliable and stable [1]. Elliptic or so-called Cauer filters represent a specific type of LC ladder filters having the transmission zeros as well as poles at finite frequencies that create equal-ripple variations in both the pass-band and the stop-band and feature faster transition from the pass-band to the stop-band than any other class of network synthesis filters [2]. However, on-chip spiral inductors occupy large chip area and therefore are costly and suffer from substrate resistive losses and capacitive couplings. Moreover, their value in passive form is not easily tunable [3]. Due to these disadvantages, after introducing active filters, it has become a common practice to reproduce the operation of ladder passive filters by means of active filter counterparts to maintain the same low-sensitivity characteristics. One of the most powerful methods for synthesis of LC ladder filters is the linear transformation (LT) technique. The principle is based on the linear transformation of port variables of a network from the *V-I* domain to a new domain, in which active realizations are effected [4], [5]. In other words, LT active filters realize systematic design tables i.e. every section of the original ladder prototype is realized by using active building blocks (ABBs) individually. In general, in the open literature this design technique has been firstly applied using operational amplifiers (OAs) [4], however, due to smaller dynamic range, narrow bandwidth, and higher power consumption of OAs, also on various recently introduced non-conventional high performance ABBs. In open literature various third-order low-pass filter (LPF) realizations exist [6]–[13], however this paper is strictly focused on active only grounded-C third-order voltage-mode (VM) elliptic LPF design [10]–[13]. Therefore, for fair comparison of here presented solution the operational transconductance amplifier (OTA) [10] and second-generation current conveyors (CCIIs)-based solutions are relevant [11], [12]. Both OTA and CCII are suitable for LT filter synthesis, because they have high-impedance input. In [10], the active only grounded-C realization employs seven OTAs, while in [11] and [12] six CCIIs, three voltage followers, six resistors (including floating ones), and five CCIIs and six grounded resistors are used, respectively. In [13], the signal flow graph (SFG) approach [14] was used for third-order elliptic LPF design. Here, the original ladder network is divided into subsections and then using SFG each subsection is realized one by one. Hence the low sensitivity basis is guaranteed while reducing the complexity of a large signal flow graph diagrams. On the other hand, although both methods are attractive for third-order elliptic LPF design, none of these two methods consider filter structure

Manuscript received January 8, 2015; accepted March 22, 2015.
Research described in this paper was financed by the National Sustainability Program under grant LO1401. For the research, infrastructure of the SIX Center was used.

optimization. Therefore, the main aim of this paper is to combine both LT technique and SFG approach such that firstly the active only grounded-C equivalent of third-order VM elliptic LPF is simply designed by LT, i.e. by replacement of passive components by theirs active equivalents and the SFG approach is with advantage used as powerful tool for the LT structure optimization.

The paper is organized as follows: Section II describes the recently introduced ABB so-called current follower transconductance amplifier (CFTA), which is in this paper used for filter design. Part of this section also shortly deals with the Mason-Coates' SFGs definition and evaluation. In section II-C the CFTA-based new active only grounded-C third-order VM elliptic low-pass filter and its optimized circuit solution are presented. Section III discusses experimental verification, while IV concludes the paper.

II. CIRCUIT DESCRIPTION

A. Description of CFTA+/

In several earlier reported circuits the potential of the CDTA was not fully used, since one of the input terminals p or n of input sub-block current differencing unit (CDU) is not connected into the proposed function block [15] [21]. Thus, this may cause some noise injection into the IC circuit. Hence, in order to prevent this potential drawback of future applications, the CFTA was introduced as novel ABB for analog signal processing in 2008 [22] [26]. The CFTA+/ is a four-terminal ABB, which circuit symbol and behavioural model are shown in Fig. 1. Basically, it consists of an input positive current follower stage, which transfers the input current i_f to the z terminal and an OTA stage that converts the voltage at the z terminal to output currents at the x+ and x terminals. Using standard notation, the relationship between port currents and voltages of non-ideal CFTA+/ can be described by the following hybrid matrix:

$$\begin{bmatrix} i_z \\ i_{x+} \\ i_{x-} \\ v_f \end{bmatrix} = \begin{bmatrix} Y_z & 0 & 0 & \alpha(s) \\ g_m(s) & Y_{x+} & 0 & 0 \\ -g_m(s) & 0 & Y_{x-} & 0 \\ Z_f & 0 & 0 & 0 \end{bmatrix} \begin{bmatrix} v_z \\ v_{x+} \\ v_{x-} \\ i_f \end{bmatrix}, \quad (1)$$

where the $g_m(s)$ and $\alpha(s)$ represent frequency dependent transconductance gain from the z terminal to x+ and x terminals and frequency dependent non-ideal current gain, respectively. The $Z_f = R_f$ is parasitic intrinsic input resistance and $Y_k = sC_k + 1/R_k$ for k ∈ {z, x+, and x } are parasitic admittances at corresponding terminals of CFTA+/ , respectively. Note that in ideal case the current gain is unity, i.e. $\alpha(s) = 1$, and frequency independent.

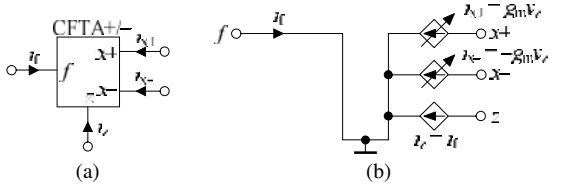

Fig. 1. Circuit symbol (a), behavioural model of CFTA+/ (b).

Using a single-pole model it can be defined as $\alpha(s) = \alpha_o/(1 + \tau_a s)$, where α_o is dc current gain, $1/\tau_a$ is bandwidth dependent on the IC fabrication of ABB, however, in current CMOS or BiCMOS technologies the bandwidth is in order of a few Grad/s. Hence, at low and medium frequencies, i.e. $f \ll (1/(2\pi)) \times \min\{1/\tau_a\}$, the frequency dependent current gain $\alpha(s)$ turns to $\alpha(s) \cong \alpha_o = 1 + \varepsilon_{ai}$, whereas ε_{ai} is current tracking error and satisfies $|\varepsilon_{ai}| \ll 1$. It should be also mentioned that depending on specific implementation of the CFTA+/ its above mentioned parasitic intrinsic input resistance and non-ideal current gain can be with advantage used as current-controlled tunable parameters. In such cases the current-controlled and/or controlled-gain CFTA could be elaborated.

B. Mason-Coates' Signal Flow Graphs

For the design and optimization of the active frequency filters based on the passive prototype, the SFG approach has been used. To be able to follow the design and optimization steps the following paragraph shortly describes the evaluation of the transfer function of an M-C (Mason-Coastes) SFG.

It is known that the transfer function of an M-C SFG can be determined using the equation also labelled as Mason's gain formula [14]

$$K = \frac{Y}{X} = \frac{1}{\Delta}\sum_i P_i \Delta_i, \quad (2)$$

where P_i is the transfer of the ith direct path from the input current or voltage node X to the output current and voltage node Y, and Δ is the determinant of a graph that is given as follows

$$\Delta = V - \sum_k S_1^{(k)} V_1^{(k)} + \sum_l S_2^{(l)} V_2^{(l)} - \sum_m S_3^{(m)} V_3^{(m)} + \ldots, \quad (3)$$

where V is the product of the self-loops, $S_1^{(k)}$ is the transfer of the kth oriented loop, and $V_1^{(k)}$ is the product of all self-loops not-touching the kth oriented loop, $S_2^{(l)}$ is the transfer product of two not-touching oriented loops, and $V_2^{(l)}$ is the product of the self-loops not-touching the lth oriented loops. If an oriented loop or kth direct path is touching all nodes, then the product V or Δ_k is unity. In (2), Δ_i is the determinant of that part of the graph that is not touching the i-th direct path.

Except the knowledge of evaluating the transfer function of an M-C graph, using the flow graph theory for synthesis of circuits, also the corresponding M-C graph of the active element must be known. According to (1) the corresponding M-C graph of an ideal CFTA+/ active element is shown in Fig. 2.

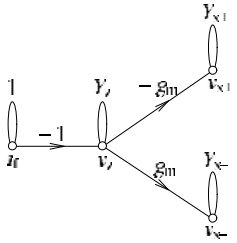

Fig. 2. Reduced M-C flow graph of CFTA+/ .

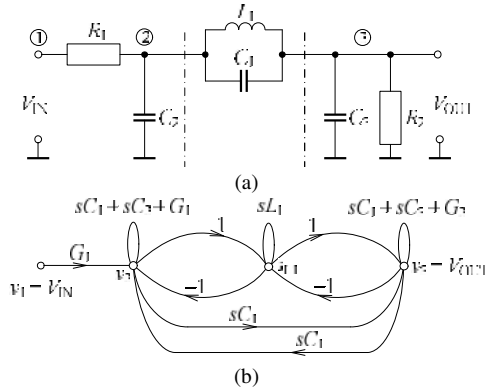

Fig. 3. Third-order passive LC ladder filter prototype (a), corresponding M-C graph (b).

C. The Passive Frequency Filter Prototype, its New Active Equivalents, and Optimization

As mentioned above, the proposed active only CFTA-C frequency filter is based on the passive LC ladder prototype, which is shown in Fig. 3(a). This circuit represents a third-order elliptic LPF with the voltage transfer function

$$K_{\text{pas}} = \frac{s^2 L_1 C_1 + G_1}{s^3 a_3 + s^2 a_2 + s a_1 + a_0}, \tag{4}$$

where $a_0 = G_1 + G_2$, $a_1 = C_2 + C_3 + L_1 G_1 G_2$, $a_2 = L_1\left[C_1\left(G_1 + G_2\right) + G_1 C_3 + G_2 C_2\right]$, and $a_3 = L_1\left[C_1 C_2 + C_3\left(C_1 + C_2\right)\right]$.

The equivalent M-C graph of the passive LC ladder filter from Fig. 3(a) is shown in Fig. 3(b). Replacing resistors R_1 and R_2, floating capacitor C_1 and inductor L_1 in the passive prototype (Fig. 3(a)) by their corresponding representations employing only CFTAs as active elements and/or capacitors [26], the CFTA-C frequency filter realization is obtained as shown in Fig. 4(a). The corresponding M-C flow graph of this solution is shown in Fig. 4(b) and can be used to evaluate the voltage transfer function, which has a form

$$K_{\text{act}} = \frac{s^2 C_{\text{L1}} C_{\text{C1}} g_{\text{m1}} g_{\text{m3}} + g_{\text{m1}} g_{\text{m3}} g_{\text{m6}} g_{\text{m7}}}{s^3 b_3 + s^2 b_2 + s b_1 + b_0}, \tag{5}$$

where $b_3 = C_{\text{L1}}\left(C_{\text{C1}} C_2 g_{\text{m5}} + C_2 C_3 g_{\text{m7}} + C_{\text{C1}} C_3 g_{\text{m3}}\right)$,
$b_2 = C_{\text{L1}}\left[C_{\text{C1}}\left(g_{m3} g_{\text{m8}} + g_{\text{m2}} g_{\text{m5}}\right) + g_{\text{m7}}\left(C_3 g_{\text{m2}} + C_2 g_{m7}\right)\right]$,
$b_1 = g_{\text{m7}}\left(C_3 g_{\text{m3}} g_{\text{m4}} + C_2 g_{\text{m4}} g_{\text{m5}} + C_{\text{L1}} g_{\text{m2}} g_{\text{m8}}\right)$, and
$b_0 = g_{\text{m4}} g_{\text{m7}}\left(g_{\text{m2}} g_{\text{m5}} + g_{\text{m3}} g_{\text{m8}}\right)$.

Comparing the transfer functions (4) and (5), the active only grounded-C third-order VM elliptic LPF from Fig. 4(a) generally provides the third-order elliptic low-pass response as required. However, as it can be evident, by simple interconnection of corresponding active replacements of replaced passive elements, the proposed filter is quite excessive in the required number of active elements point of view. Therefore, optimization steps can be done that lead to reducing the number of active elements in the final active CFTA-C third-order VM elliptic low-pass filter solution.

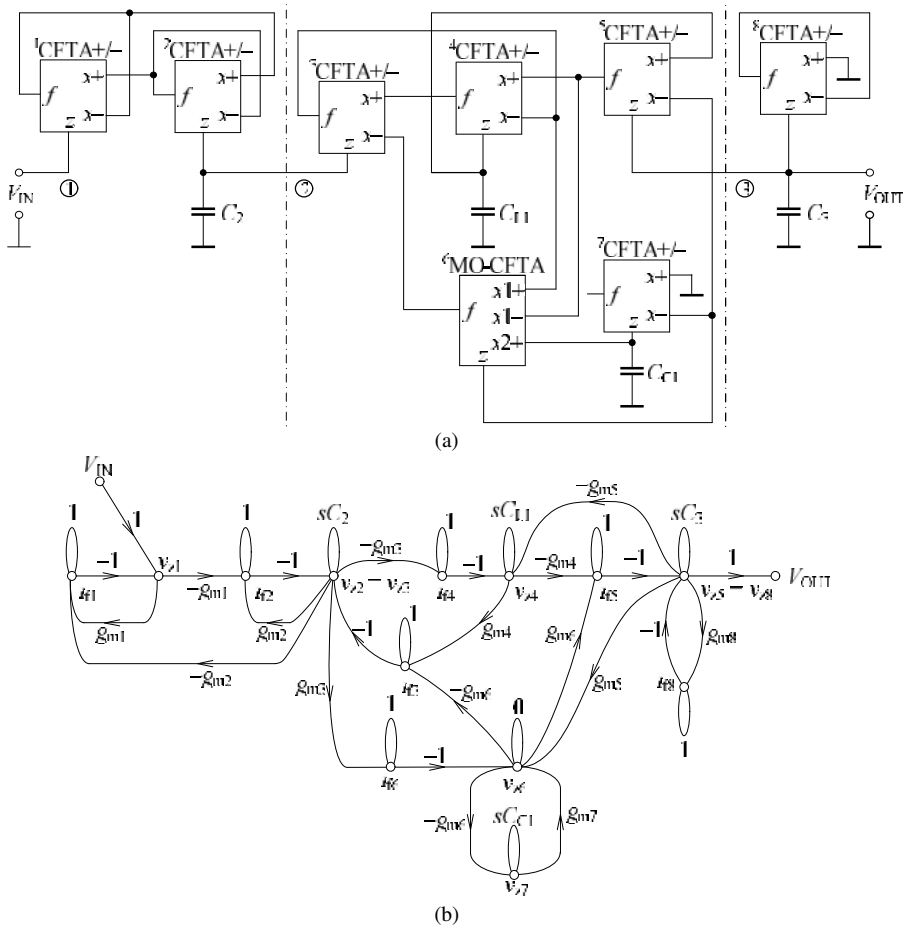

Fig. 4. Equivalent third-order VM elliptic low-pass filter (a) and its corresponding M-C signal flow graph (b).

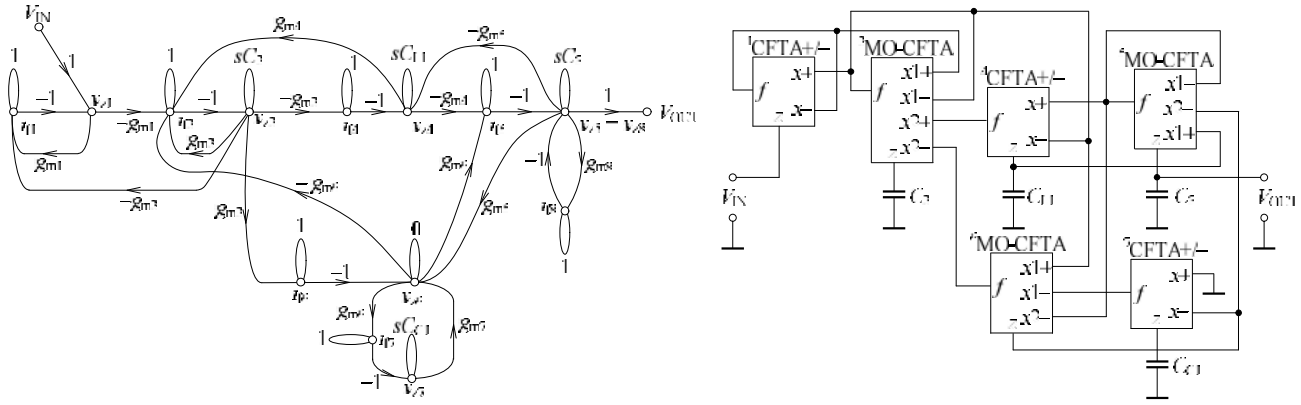

Fig. 5. Optimized M-C signal flow graph (a), corresponding active only grounded-C third-order VM elliptic low-pass filter (b).

To follow the optimization steps, the numbering of main active elements remains the same. Using an additional current output x in [5]MO-CFTA (multi-output CFTA), the [8]CFTA+/ in the original solution given in Fig. 4(a) can be omitted in a very simple way as it can be seen from Fig. 5(a) showing the optimized circuit solution. Similarly, the [2]CFTA+/ and [3]CFTA+/ in the original solution can be joined, where in the optimized circuit only the [2]MO-CFTA is presented featuring multiple current outputs x+ and x–. In order to prevent potential noise injection into the on-chip circuit or fabricated prototype, the final optimization step consists in employing the f terminal of [7]CFTA+/ . To ensure that the transfer function does not chance, x_{2-} current output of [6]MO-CFTA must be used.

The transfer function of the optimized active only grounded-C third-order VM elliptic low-pass filter can be expressed as

$$K_{\text{act\_opt}} = \frac{s^2 C_{\text{L1}} C_{\text{C1}} g_{\text{m1}} g_{\text{m2}} + g_{\text{m1}} g_{\text{m2}} g_{\text{m4}} g_{\text{m7}}}{s^3 c_3 + s^2 c_2 + s c_1 + c_0}, \quad (6)$$

where $c_3 = C_{\text{L1}}\left(C_{\text{C1}} C_3 g_{\text{m2}} + C_2 C_3 g_{\text{m7}} + C_2 C_{\text{C1}} g_{\text{m5}}\right)$,

$c_2 = C_{\text{L1}}\left[2C_{\text{C1}} g_{\text{m2}} g_{\text{m5}} + g_{\text{m7}}\left(C_3 g_{\text{m2}} + C_2 g_{\text{m5}}\right)\right]$,

$c_1 = g_{\text{m7}}\left(C_2 g_{\text{m4}} g_{\text{m5}} + C_3 g_{\text{m2}} g_{\text{m4}} + C_{\text{L1}} g_{\text{m2}} g_{\text{m5}}\right)$,

$c_0 = 2 g_{\text{m2}} g_{\text{m4}} g_{\text{m5}} g_{\text{m7}}$.

Comparing the transfer functions (6) and (4), the optimized structure of active CFTA-C filter from Fig. 5(b) also provides the third-order elliptic low-pass response as required and hence the optimization steps are correct. In addition, after the optimization steps, the number of active elements compared with the first CFTA-C filter realization shown Fig. 4(a) was reduced by two, which may reduce its chip area in case of on-chip fabrication.

III. MEASUREMENT RESULTS

In order to confirm the theoretical study and to show the performance of the optimized active only grounded-C third-order VM elliptic LPF from Fig. 5(b), its behaviour has been verified by experimental measurements. To implement the CFTA+/ and MO-CFTAs, the readily available UCC-N1B integrated circuit (IC) developed in the CMOS 0.35 μm technology, which implements the universal current conveyor (UCC) and second-generation current conveyor CCII+/–, has been used [27], [28]. The realization of the MO-CFTA by means of UCC-N1B is shown in Fig. 6, where the grounded resistor R_K defines the transconductance of the active element, whereas $g_m = 1/R_K$.

The third-order elliptic low-pass filter [29] was designed with the following specification: cut-off frequency 110 kHz, stopband frequency 205 kHz, passband ripple 1 dB, and minimum stopband attenuation 30 dB. The passive element values in the optimized version of the proposed active only CFTA-C third-order VM elliptic LPF from Fig. 5(b) have been determined as follows: $C_{C1} = 3.9$ nF, $C_{L1} = 3.9$ nF, $C_2 = C_3 = 27$ nF, and $g_{mi} = 1/R_{Ki} = 1/100\ \Omega$ for $i \in$ (1, 2, 4, 5, 6, and 7). The developed PCB (printed circuit board) is shown in Fig. 7and the experimental measurements have been carried out using network-spectrum analyser Agilent 4395A.

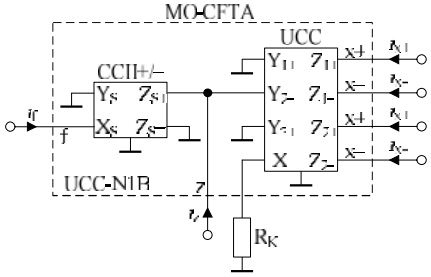

Fig. 6. MO-CFTA realization using UCC-N1B integrated circuit.

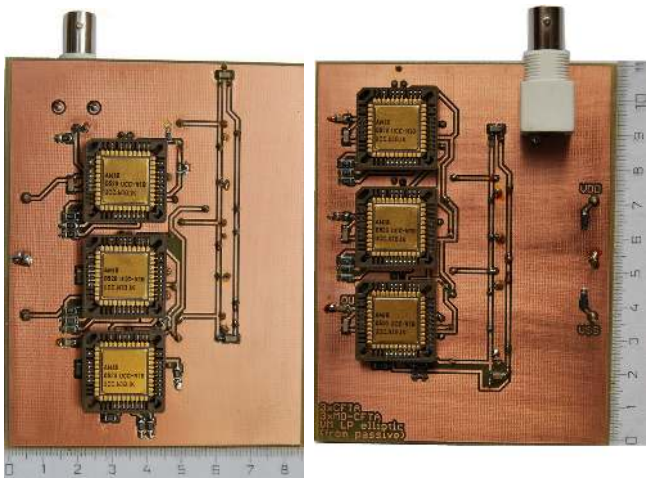

Fig. 7. The PCB prototype of the proposed grounded-C third-order VM elliptic low-pass filter from Fig. 5(b) (the PCB size is given in cm).

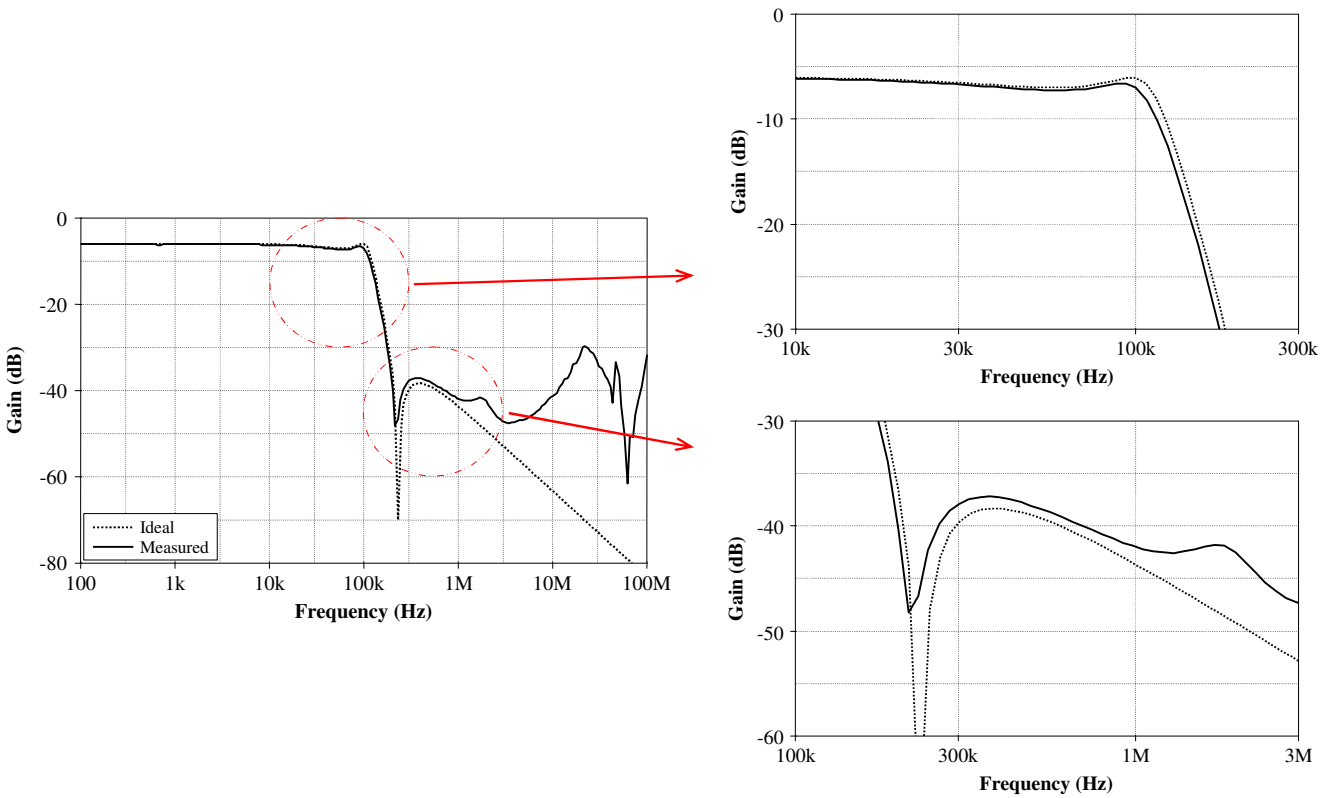

Fig. 8. Ideal and measured gain characteristics of the optimized grounded-C third-order VM elliptic low-pass filter from Fig. 5(b).

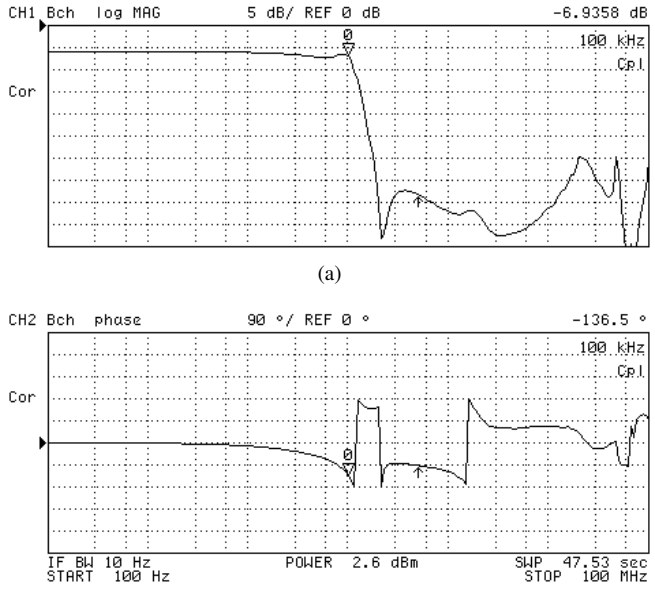

Fig. 9. Measured gain (a) and phase (b) characteristics of the optimized grounded-C third-order VM elliptic low-pass filter from Fig. 5(b).

Both ideal and measured gain responses are shown and compared in Fig. 8. In addition, the screenshot from the network-spectrum analyser showing measured gain and phase responses are given in Fig. 9. The value of the cut-off frequency determined from measurements is approx. 98 kHz. The decrease in the cut-off frequency is caused by the parameters of the used UCC-N1B ICs [27], [28], however, the real behaviour of the filter is still very satisfactory and experimental results confirm the theoretical study.

IV. CONCLUSIONS

In this paper, the Mason-Coates' signal flow graph approach is demonstrated as powerful tool for third-order voltage-mode elliptic LPF optimization. First, the number of active elements was reduced by two. Second, the not connected low-impedance input terminal was eliminated preventing potential noise injection into the fabricated PCB during experiments. The designed CFTA-based final solution is the first third-order VM elliptic low-pass filter in the open literature. From the experimental results it can be observed that the cut-off frequency precisely agrees to theoretically predicted one. Note that the in higher frequency region the filter characteristics are partly affected by the real properties of the used ICs. However, since the attenuation in full frequency range is below 30 dB, the results are really favourable.

REFERENCES

[1] R. Raut, M. N. S. Swamy, *Modern Analog Filter Analysis And Design: A Practical Approach*. Wiley-VCH Verlag & Co. KGaA, Germany, ch. 7, 2010.

[2] K. Su, *Anlog Filters*. Kluwer Academic Publishers, Dordrecht, ch. 2, 2003.

[3] G. Thanachayanont, A. Payne, "CMOS floating active inductor and its applications to bandpass filter and oscillator designs", *IEE Proc.-Circuits Devices Systems*, 2000, vol. 147, no. 1, pp. 42–48. [Online]. Available: http://dx.doi.org/10.1049/ip-cds:20000053

[4] A. G. Constantinides, H. G. Dimopoulos, "Active RC filters derivable from LC ladder filters via linear transformations", *IEE J. Electronic Circuits and Systems*, vol. 1, no. 1, pp. 17–21, 1976. [Online]. Available: http://dx.doi.org/10.1049/ij-ecs.1976.0005

[5] H. G. Dimopoulos, A. G. Constantinides, "Linear transformation active filters", *IEEE Trans. Circuits and Systems*, vol. 25, no. 10, pp. 845–852, 1978. [Online]. Available: http://dx.doi.org/10.1109/S.1978.1084391

[6] M. Somdunyakanok, K. Angkeaw, P. Prommee, "Floating-capacitance multiplier based on CCDDCCs and its application", in *Proc. IEEE Region 10 Conf. TENCON 2011*, Bali, 2011, pp. 1367–1370. [Online]. Available: http://dx.doi.org/10.1109/TENCON.2011.6129031

[7] N. Krishnapura, A. Agrawal, S. Singh, "A high-IIP3 third-order elliptic filter with current-efficient feedforward-compensated opamps", *IEEE Trans. on Circuits and Systems II*, vol. 58, no. 4, pp. 205–209, 2011. [Online]. Available: http://dx.doi.org/10.1109/TCSII.2011.2124571

[8] C. Garcia-Alberdi, A. J. Lopez-Martin, L. Acosta, R. G. Carvajal, J. Ramirez-Angulo, "Tunable class AB CMOS gm-C filter based on quasi-floating gate techniques", *IEEE Trans. on Circuits and Systems I*, vol. 60, no. 5, pp. 1300–1309, 2013. [Online]. Available: http://dx.doi.org/10.1109/TCSI.2012.2220504

[9] A. Guney, H. Kuntman, "New floating inductance simulator employing a single ZC-VDTA and one grounded capacitor", in *Proc. 2014 9th IEEE Int. Conf. Design & Technology of Integrated Systems In Nanoscale Era (DTIS)*, Santorini, Greece, 2014, pp. 1–2. [Online]. Available: http://dx.doi.org/10.1109/DTIS.2014.6850643

[10] Y.-S. Hwang, S.-I. Liu, D. S. Wu, Y.-P. Wu, "Table-based linear transformation filters using OTA-C techniques", *Electronics Letters*, vol. 30, no. 24, pp. 2021–2022, 1994. [Online]. Available: http://dx.doi.org/10.1049/el:19941414

[11] Y.-S. Hwang, P.-T. Hung, W. Chen, S.-I. Liu, "CCII-based linear transformation elliptic filters", *International Journal of Electronics*, vol. 89, no. 2, pp. 123–133, 2002. [Online]. Available: http://dx.doi.org/10.1080/00207210110105181

[12] Y.-S. Hwang, P.-T. Hung, W. Chen, S.-I. Liu, "Systematic generation of current-mode linear transformation filters based on multiple output CCIIs", *Analog Integrated Circuits and Signal Processing*, vol. 32, no. 2, pp. 123–134, 2002. [Online]. Available: http://dx.doi.org/10.1023/A:1019521925527

[13] A. Jiraseree-amornkun, W. Surakampontorn, "Efficient implementation of tunable ladder filters using multi-output current controlled conveyors", *AEU - International Journal of Electronics and Communications*, vol. 62, no. 1, pp. 11–23, 2008. [Online]. Available: http://dx.doi.org/10.1016/j.aeue.2007.01.005

[14] W. K. Chen, *The Circuits and Filters Handbook*. New York: CRC Press, 2003.

[15] D. Biolek, "CDTA - building block for current-mode analog signal processing", in *Proc. 16th ECCTD*, Krakow, Poland, 2003, pp. 397–400.

[16] W. Tangsrirat, W. Surakampontorn, "Systematic realization of cascadable current-mode filters using current differencing transconductance amplifiers", *Frequenz*, vol. 60, no. 11–12, pp. 241–245, 2006. [Online]. Available: http://dx.doi.org/10.1515/FREQ.2006.60.11-12.241

[17] A. U. Keskin, D. Biolek, E. Hancioglu, V. Biolkova, "Current-mode KHN filter employing current differencing transconductance amplifiers", *AEU - International Journal of Electronics and Communications*, vol. 60, pp. 443–446, 2006. [Online]. Available: http://dx.doi.org/10.1016/j.aeue.2005.09.003

[18] D. Biolek, V. Biolkova, Z. Kolka, "Current-mode biquad employing single CDTA", *Indian Journal of Pure and Applied Physics*, vol. 47, no. 7, pp. 535–537, 2009.

[19] A. Lahiri, "Novel voltage/current-mode quadrature oscillator using current differencing transconductance amplifier", *Analog Integrated Circuits and Signal Processing*, vol. 61, no. 2, pp. 199–203, 2009. [Online]. Available: http://dx.doi.org/10.1007/s10470-009-9291-0

[20] J. Jin, "Resistorless active SIMO universal filter and four-phase quadrature oscillator", *Arabian Journal for Science and Engineering*, vol. 39, no. 5, pp. 3887–3894, 2014. [Online]. Available: http://dx.doi.org/10.1007/s13369-014-0985-y

[21] E. Alaybeyoglu, A. Guney, M. Altun, H. Kuntman, "Design of positive feedback driven current-mode amplifiers Z-Copy CDBA and CDTA, and filter applications", *Analog Integrated Circuits and Signal Processing*, vol. 81, no. 1, pp. 109–120, 2014. [Online]. Available: http://dx.doi.org/10.1007/s10470-014-0345-6

[22] N. Herencsar, J. Koton, I. Lattenberg, K. Vrba, "Signal-flow graphs for current-mode universal filter design using current follower transconductance amplifiers (CFTAs)", in *Proc. APPEL 2008*, Pilsen, Czech Republic, 2008, pp. 69–72.

[23] N. Herencsar, J. Koton, K. Vrba, I. Lattenberg, "Novel SIMO type current-mode universal filter using CFTAs and CMIs", in *Proc. 31st TSP 2008*, Paradfurdo, Hungary, 2008, pp. 107–110.

[24] N. Herencsar, K. Vrba, J. Koton, A. Lahiri, "Realisations of single-resistance-controlled quadrature oscillators using generalised current follower transconductance amplifier and unity-gain voltage-follower", *International Journal of Electronics*, vol. 97, no. 8, pp. 897–906, 2010. [Online]. Available: http://dx.doi.org/10.1080/00207211003733320

[25] N. Herencsar, J. Koton, K. Vrba, "Realization of current-mode KHN-equivalent biquad using current follower transconductance amplifiers (CFTAs)", *IEICE Trans. Fundamentals*, vol. E93-A, no. 10, pp. 1816–1819, 2010. [Online]. Available: DOI: http://dx.doi.org/10.1587/transfun.E93.A.1816

[26] J. Koton, N. Herencsar, M. Venclovsky, "History, progress and new results in synthetic passive element design employing CFTAs", *International Journal of Advances in Telecommunications, Electrotechnics, Signals and Systems*, vol. 4, no. 1, pp. 15-26, 2015. [Online]. Available: http://dx.doi.org/10.11601/ijates.v4i1.113

[27] Datasheet UCC-N1B-IK – Prototype of the integrated circuit: universal current conveyor UCC & second generation current conveyor CCII+/ . ON Semiconductor & BUT Brno, UCC_N1B_Rev0, 2010.

[28] J. Jerabek, K. Vrba, "SIMO type low-input and high-output impedance current-mode universal filter employing three universal current conveyors", *AEU - International Journal of Electronics and Communications*, vol. 64, no. 6, pp. 588–593, 2010. [Online]. Available: http://dx.doi.org/10.1016/j.aeue.2009.03.002

[29] R. W. Daniels, *Approximation Methods for Electronic Filter Design: With Applications to Passive, Active and Digital Networks*. McGraw-Hill: the University of Michigan, 1974.